Introduction to the geology and mineralogy of pegmatites located south of Mashhad (first report of Li-bearing pegmatites from Iran)

Pezhvak Didar[1*], Mohammad Hashem Emami[2], Fatemeh Emamian[3]

1- Geological Research Center of Geological Survey of Iran.
2- Islamic Azad University, Eslamshahr Branch, Eslamshahr, Iran.
3- Geological Survey of Iran, Tehran, Iran.

* Corresponding Author: pezhwakdidar@gmail.com

Received: 28 January, 2015 / Accepted: 14 March 2015 / Published online: 15 May 2015

Abstract

The granites south of Mashhad are located in the north-east of Iran and occur in the suture zone between the Binalud and Kopeh Dagh areas. These S-type granites are peraluminous with an Upper Triassic Age and include intersecting pegmatites. These pegmatites are homogenous and show simple mineralogical combinations which include K-feldspars (microcline and orthoclase), plagioclase, quartz, micas (biotite, muscovite and lepidolite), tourmaline (elbaite, dravite, and schorl) and garnet (almandine-spessartite). The pegmatites south of Mashhad belong to the LCT (Lithium-Cesium-Tantalum) and MSREL-Li (Muscovite- REE-Li).The Li-content of these pegmatites ranges between 202-1653 ppm and the ratios K/Cs, K/Rb and Al/Ga are high which indicates a low level of differentiation. The Mg/ Li ratio in these pegmatites lies between 0.2-12.6. All the element ratios indicate that pegmatites are low evolved.

Keywords: Pegmatite, Lepidolite, Lithium, Mashhad, Iran.

1–Introduction

Nowadays lithium and its derivatives (compounds) have vast applications in the technology and industry including their use in lithium batteries, ceramics, glazes, fluxes, electrolysis etc. Pegmatites are one of the most important sources for extraction of lithium. The important lithium–bearing minerals present in the pegmatites are: spodumene, lepidolite, petalite and amblygonite. Fertile S-type, peraluminous granites produce LCT (Lithium-Cesium-Tantalum) pegmatites which are generated by the partial melting (anatexis) of the Upper/Middle Crust rocks. In most areas the LCT type pegmatite is enriched in Li and it constitutes the most suitable source for the extraction of Li (Černý, 1989). In general, pegmatites are homogeneous or heterogeneous with respect to their mineralogical composition. Homogeneous pegmatites are not of remarkable value except in some cases where they are exploited for lithium, feldspar or micas (Guilbert and Park, 1986).

The granites of South Mashhad in north-east Iran include discordant pegmatites. Although many studies have been carried out on these granites, the associated pegmatites have not been specifically described nor has their mineralization (especially with respect to Li) been reported. In this paper, lithium- bearing mineralization is described for the first time in Iran. In view of the increasing need of the world's industry for this strategic element, it is necessary to study these resources even if they are of low grade.

2–Analytical techniques

This study is based on an extensive field work and sampling on the granites and pegmatites of Mashhad during which one hundred large samples (at least five kilogram each) from different parts of granite and pegmatite outcrops were taken. Fluid inclusion investigations were conducted on six samples at the geological Survey of Iran, Tehran. Temperature-related phase changes were measured using a Linkam heating-freezing stage mounted on a microscope with 4, 10, 20, and 80X objectives.

Eighty thin and polished-thin sections from the rock samples were examined in transmitted and reflected light. Among them, twenty of these sections were examined (and partly photographed) for trace elements on an SEM-EDS (Microscope: ΣIGMA/VP-ZEISS and Detector: X-Max Oxford) equipped with EDX at the Center for Applied Researches of the Geological survey and Mineral Exploration of Iran, Karaj. Twenty-two samples of mica and feldspar together with seventy-two bulk samples from granites and pegmatites were prepared and analyzed for major and trace elements using ICP-OES (Varian 735-ES) at the Center for Applied Researches of the Geological Survey and Mineral Exploration of Iran, Karaj. Also eighty-six samples were investigated using XRD (Inel-EQUNOX 3000) method at the same center.

3–Geological Background

3.1- Regional Geology

The granites of South of Mashhad occur in the Mashhad Zone according to the proposed categorization of structural zones of Iran (Alavi, 1991). It is believed that the intrusives of this region have beenemplaced in the form of multiple intrusive pulses which appear to be related to the Hercynian tectonic movements and their post-tectonic phases (Emami, 2000).

The 1:100,000 Geological Map of Mashhad (Taheri and Ghaemi, 1994) comprises three distinct zonesfrom north to south which are: the Kopeh Dagh zone, the Suture Zone and the Binalud Zone (Taheri and Ghaemi, 1994). The Suture Zone lies in between the Kopeh Dagh Zone and the Binalud Zone and it includes intrusive granite bodies, Ophiolite Complex and related metamorphics which constitute linear belts with a length of tens of kilometers, trending NW-SE along the northern slopes of the Binalud Range. This zone is the junction of collision of the Iranian lithospheric plate in the south and the Turanian plate in the north which led to the closure of the Paleotethys (Alavi, 1991). The Paleotethys Suture zone lies in the Mashhad area to the north of the Binalud Range in NE Iran.

3.2- The Granites of South of Mashhad

The granites of south Mashhad, which host the pegmatites, are located in thesuture zone between the Kopeh Dagh zone and the Binaloud zone. These granites include three different intrusive phases of gr^1, gr^2, and gr^3 in an area of 40 km^2. All types of granites host pegmatites (Fig. 1).

The gr^1 granite is a peraluminous, S-type, calc-alkaline rock with a monzo- to syeno-granite composition. This granite is biotite and biotite-tourmaline bearing with hypidiomorphic porphyroblasts of feldspar. The zircon U-Pb dating of gr^1, performed by Karimpour *et al*. (2009), has revealed a 201.3±3.6 Ma age (upper Triassic), while $(^{87}Sr/^{86}Sr)_i$ and $(^{143}Nd/^{144}Nd)_i$ are 0.706776 and 0.5122219, respectively. These ratios correspond to a contaminated lower crust origin (Karimpour *et al*., 2009). The restites present in the gr^1 granite show a general trend of N35. The total amount of trace elements of the gr1 granite differs from 212 to 481ppm, where Eu indicates a negative value (Eu/Eu*=0.62-0.88) (Karimpour *et al*., 2009).

The gr^2 granite is a peraluminous, S-type, calc-alkaline rock with a monzo- to syenogranite (Muscovite and Biotite) composition and has intruded into the gr^1 granite (i.e. younger phase). This granite has been generated from the

shallower depth of continental crust during the Late Cimmerian orogenic phase (Valizadeh and Karimpour 1995; Didar, 2004). The gr^2 is distinguishable from gr^1 by lack of restite, equigranular fair grains and consequently fairer general rock color.

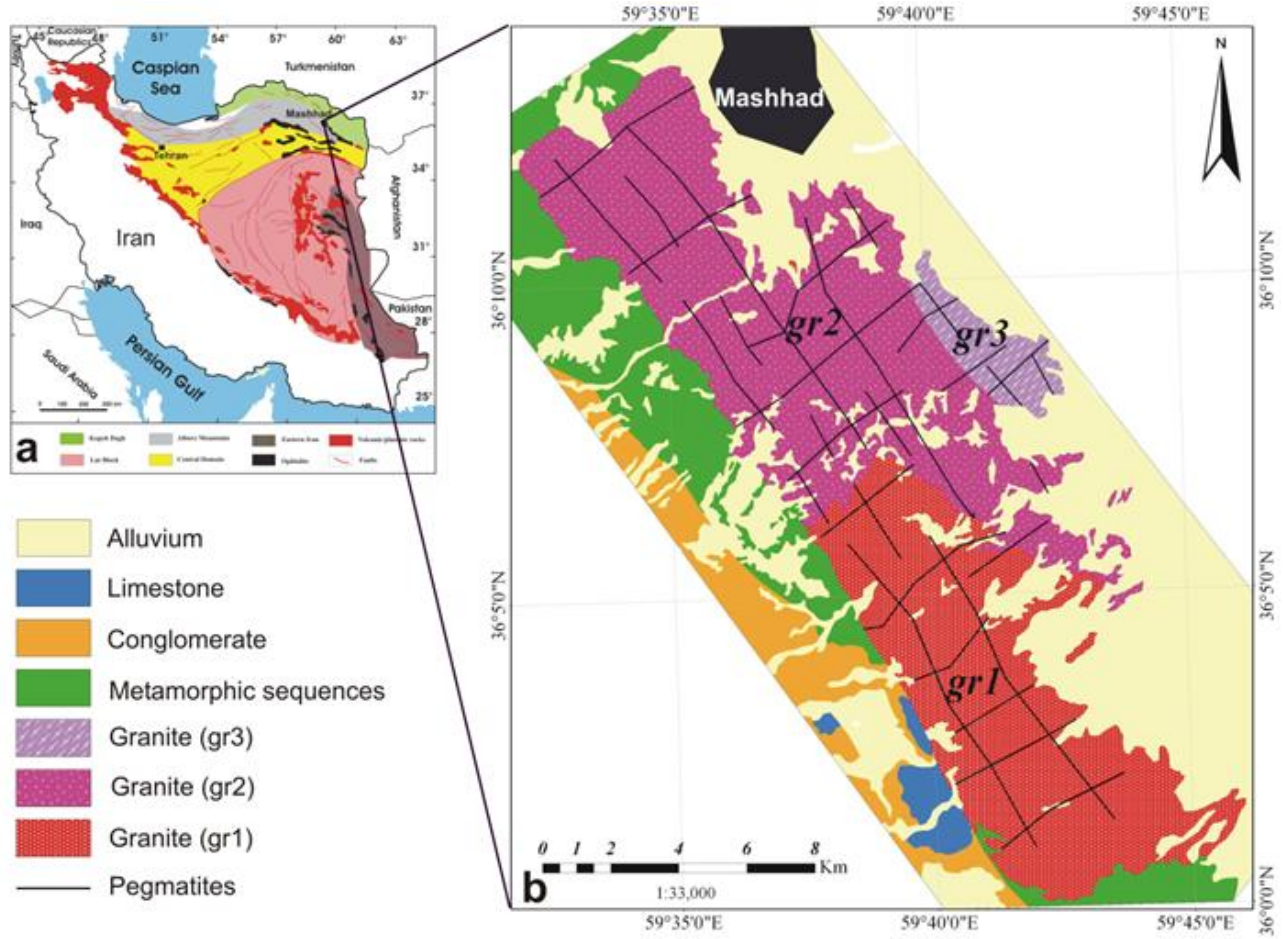

Figure 1a) Location of Mashhad in north-east Iran; b) Geological map of granites (gr^1, gr^2, gr^3) south of Mashhad, showing the location oftheirpegmatites.

The gr^3 granite is a peraluminous, S-type, calc-alkaline rock with a monzo- to syenogranite composition (muscovite and garnet bearing). This granite has been dated to 205.9±4.1 Ma (Upper Triassic) using zircon U-Pb method (Karimpour *et al*., 2011). The total amount of the REEs of this rock unit differs from 130 to 176, where Eu indicates a slight negative value (Eu/Eu*=0.52-0.76). The $(^{87}Sr/^{86}Sr)_i$ and $(^{143}Nd/^{144}Nd)_i$ of gr^3 are 0.708161 and 0.5122214, respectively, the ratios indicating a continental crust origin for the magma (Karimpour *et al*., 2011). Based on the Rb/Sr (1 to 1.3) and CaO/Na_2O (~ 0.3) of gr^3, the source rock might have been a metaplete to metapsamite (Karimpour *et al*., 2011).

In general, all the granites hosting the pegmatites (gr^1, gr^2, and gr^3 shown on the Mashhad 1:100,000 Geological Map) are silicic, peraluminous, calc-alkaline and S-type leuco-granites. The average sum of Na_2O+K_2O for these granites is about 10% and their mean K/Rb ratio ranges from 2.03 in gr^1 to 1.55 in gr^3 (Table 1). These granites fall in the "strongly evolved and fractionated region" of Blevin'sdiagram (Blevin, 2003; Fig. 2). The CaO and MgO contents are very low (≈1% and ≈0.2% respectively). The average Mg/Li ratio in these three granites ranges from 5.3 in gr^1 to 0.7 in gr^3 (Table 1). Based on the available data it can be concluded that all the three granites are fractionated and rather strongly evolved.

Table 1) Results of element analysis by ICP-OES (including elemental ratios) for granites hosting the pegmatites south of Mashhad

Sample Label	Whole Rock ICP-CES Analysis of Hosted Granites (ppm)																																				Ratio							
	Al	K	Na	Ca	Fe	Mg	Mn	Ti	P	Be	Cs	Dy	Er	Eu	Ga	Gd	Li	Nb	Nd	Sm	Te	Ge	Ce	La	Rb	Sr	Pb	Zr	V	U	Th	Y	Yb	K/Rb	K/Cs	Rb/Cs	Al/Ga	Rb/Sr	Mg/Li	Th/U	Al/CNK	K/Na	Fe/Mn
gr1-1	73127	39531	32120	17986	20721	3508	488	2022	1000	7.1	4.1	1.1	1.4	0.8	16.9	2.8	165	38.4	26.2	3.7	<0.30	0.7	73.0	42.4	195	482	346	144	27.8	12.6	13.1	13.3	1.2	202	9639	48	4320	0.4	6.7	1.0	1.2	1.2	42
gr1-2	59380	40432	32561	13808	15927	3311	300	1387	626	3.6	2.5	<0.30	0.9	0.6	13.9	2.0	107	36.3	25.9	3.2	<0.30	0.5	78.0	50.4	151	462	259	160	23.3	11.7	10.2	1.0	283	15571	48	4281	0.3	6.2	1.2	1.0	1.2	53
gr1-3	58994	37916	40392	5193	4550	484	227	241	474	26.5	1.1	<0.30	0.1	0.1	20.1	0.4	58	28.7	4.1	0.3	<0.30	<0.10	6.4	<10.0	248	82.0	12.9	84.9	4.3	16.2	4.2	2.6	0.2	153	33084	217	2935	3.0	1.7	0.3	0.9	0.8	20
gr1-4	88157	42862	41416	15075	16974	3133	495	1628	560	8.4	3.7	2.2	1.1	0.9	18.2	2.4	137	50.3	32.2	4.4	<0.30	0.3	101.6	58.7	230	629	40.6	130	28.1	14.4	14.8	1.3	187	11612	62	4737	0.4	4.6	1.0	1.3	1.0	34
Average gr1	69414	40185	39122	13017	14543	3108	378	1314	650	10.9	2.9	1.6	0.9	0.6	17.3	1.9	117	38.4	22.1	2.9	<0.30	0.5	64.7	50.5	206	434	285	130	18.9	13.7	11.8	10.2	1.0	203	17477	96	4668	0.5	5.3	0.8	1.1	1.0	39
gr2-1	85139	48992	19136	4237	9001	1494	298	908	1640	5.9	1.3	<0.30	0.7	0.4	21.7	1.9	275	36.4	22.9	3.7	<0.30	0.2	76.7	35.0	477	63.9	25.2	219	6.2	5.38	11.7	11.2	0.5	105	27400	282	3932	7.5	1.1	2.2	1.7	2.6	30
gr2-2	88721	50190	31518	9522	13152	2183	289	1239	749	7.1	2.4	1.8	0.9	0.5	18.5	2.1	215	19.0	21.7	3.8	<0.30	0.4	70.3	33.8	304	163	36.2	232	7.4	12.8	12.7	8.6	0.5	165	21327	129	4793	1.9	2.0	1.0	1.5	1.6	45
gr2-3	84380	48540	25990	9722	13962	2359	224	1528	755	5.2	2.7	2.1	0.9	0.6	19.1	2.8	148	23.4	26.1	4.9	<0.30	0.5	94.2	46.6	238	176	30.4	275	10.1	9.12	16.9	8.4	0.5	204	18003	68	4410	1.3	3.2	1.9	1.5	1.9	62
gr2-4	87713	50195	26039	4827	8457	1225	104	1311	741	3.3	1.7	2.0	0.8	0.5	18.7	1.8	142	24.6	23.2	4.2	<0.30	0.4	81.4	38.6	233	142	31.1	156	7.0	10.4	10.9	8.6	0.5	215	30234	141	4688	1.6	1.7	1.0	1.6	1.9	81
gr2-5	88840	41191	33051	6494	9688	1223	260	668	560	8.1	1.9	0.9	0.4	0.4	17.3	1.4	188	18.8	11.6	2.1	<0.30	0.2	31.5	16.0	253	101	42.6	118	4.2	12.6	7.3	8.9	0.5	183	21664	133	3973	2.5	1.3	0.6	1.3	1.2	37
gr2-6	67984	39732	28200	8564	12034	1744	207	1108	566	4.8	2.4	<0.30	0.7	0.6	18.0	1.9	173	23.1	22.2	3.9	<0.30	0.3	64.1	33.1	238	165	34.3	150	5.2	10.9	11.1	7.8	0.4	183	16728	99	3776	1.4	2.0	1.0	1.3	1.4	58
gr2-7	71383	39668	27672	6423	9328	1269	263	674	596	6.6	1.9	<0.30	0.4	0.4	17.4	1.4	178	22.5	11.3	2.2	<0.30	0.3	30.7	15.6	258	99.5	34.3	111	4.3	10.1	6.6	6.5	0.5	154	21129	137	4095	2.6	1.4	0.7	1.5	1.4	35
gr2-8	71421	46153	33143	10255	11344	1833	220	1086	708	7.5	2.4	0.8	0.7	0.4	18.7	1.8	206	19.9	15.7	3.8	<0.30	0.2	57.2	29.7	257	157	34.3	186	7.1	14.0	12.0	7.7	0.5	180	19606	109	3822	1.6	1.8	0.9	1.2	1.4	51
gr2-9	70931	43954	29809	11621	12112	2073	233	1230	645	4.4	2.5	0.7	0.7	0.6	17.3	1.9	167	22.9	22.4	4.0	<0.30	0.3	67.7	35.3	211	184	34.0	161	7.4	12.4	11.2	7.2	0.5	203	17710	85	4106	1.1	2.5	0.9	1.2	1.5	52
gr2-10	67080	39808	25862	5164	6789	849	771	306	381	7.0	1.3	<0.30	0.3	<0.10	15.5	1.0	151	31.3	5.2	0.7	<0.30	0.2	13.3	<10.0	275	56.3	26.2	91.5	2.6	12.6	5.2	10.5	1.1	145	30481	210	4319	4.9	1.1	0.4	1.2	1.1	9
gr2-11	57617	34904	28449	6475	5352	844	228	363	290	8.3	1.2	<0.30	0.2	0.2	17.7	0.8	73	44.0	8.8	1.3	<0.30	<0.10	21.9	12.8	214	93.4	27.4	84.9	3.7	10.8	5.6	8.6	0.8	163	27956	172	3257	2.3	2.3	0.5	1.2	1.2	23
gr2-12	88999	93466	22334	7473	1205	95	158	18.8	357	2.8	0.3	<0.30	<0.10	<0.10	14.0	<0.30	32	5.4	1.2	<0.30	<0.30	0.1	0.7	<10.0	1084	17.9	27.8	13.5	<2.00	7.31	0.9	0.7	<0.20	86	103951	1204	6372	60.5	0.6	0.1	1.1	4.2	8
gr2-13	77763	44023	38556	7206	9111	1262	192	514	822	6.1	1.9	1.3	0.4	0.2	16.8	1.1	225	27.1	5.6	1.4	<0.30	0.3	12.1	<10.0	248	67.4	39.5	73.8	4.2	14.3	4.5	6.4	0.5	177	23753	134	4625	3.7	1.1	0.3	1.3	1.1	47
gr2-14	76563	47816	29086	7722	11747	1539	328	965	754	7.3	2.2	<0.30	0.6	0.4	17.7	1.8	193	22.3	16.4	3.2	<0.30	0.3	54.5	27.3	292	128	31.7	168	5.6	11.5	10.8	6.3	0.3	164	21957	134	4434	2.3	1.6	0.9	1.4	1.6	36
Average gr2	78182	47824	28268	7561	9520	1429	270	848	683	6.0	1.9	1.4	0.6	0.4	17.7	1.7	166	24.3	15.9	3.0	<0.30	0.3	48.3	29.4	327	115	32.5	146	5.8	11.0	9.1	8.3	0.5	164	28700	217	4329	2.8	1.7	0.8	1.4	1.6	35
gr3-1	86722	41717	39347	6713	7584	618	133	136	814	4.8	1.5	<0.30	0.2	<0.10	19.9	0.7	165	35.5	11	<0.30	<0.30	0.3	1.4	<10.0	256	21.1	28.0	38.5	<2.00	14.6	3.1	5.5	0.4	163	25958	160	4352	12.2	0.7	0.2	1.5	1.1	57
gr3-2	86852	15577	50488	4913	10783	368	4031	34.7	300	8.8	2.3	0.5	0.2	<0.10	17.7	1.0	29	11.9	1.4	0.4	<0.30	0.4	4.6	<10.0	113	13.9	14.9	129	2.1	16.9	5.7	21.0	1.8	133	6881	10	4920	8.2	2.5	0.3	1.8	0.3	3
gr3-3	78373	48154	25320	5637	5069	369	344	156	365	10.7	1.1	<0.30	0.1	0.1	14.5	0.7	74	11.1	3.1	0.6	<0.30	0.3	7.0	<10.0	267	42.7	43.5	73.8	<2.00	13.0	3.6	7.7	0.7	181	44809	249	5391	6.2	1.0	0.3	1.3	1.4	15
gr3-4	84323	37164	47600	9283	4900	445	501	141	491	6.4	1.1	<0.30	0.2	<0.10	20.0	0.5	217	26.0	2.6	<0.30	<0.30	<0.10	3.8	<10.0	267	19.4	17.3	37.5	<2.00	17.4	3.1	8.1	0.7	139	33835	243	4213	13.8	0.4	0.2	1.3	0.8	10
Average gr3	84067	35653	43181	6637	7084	450	1252	117	494	7.7	1.5	0.5	0.2	0.1	18.0	0.7	122	21.1	2.0	0.5	<0.30	0.3	4.2	<10.0	226	24.3	25.9	69.7	2.1	15.5	3.9	10.6	0.9	155	27881	175	4719	9.3	0.7	0.2	1.5	0.8	6

3.3–The field features of the granites

Pegmatite veins cross-cut all the three phases of granites occurring south of Mashhad. The density and frequency of occurrence of pegmatites increases from gr^1 to gr^3. Furthermore, their widths also show a similar tendency. from a width of several centimeters in gr^1 to about half a meter to several meters widein gr^3 (occasionally up to 150m) running up to several kilometers.

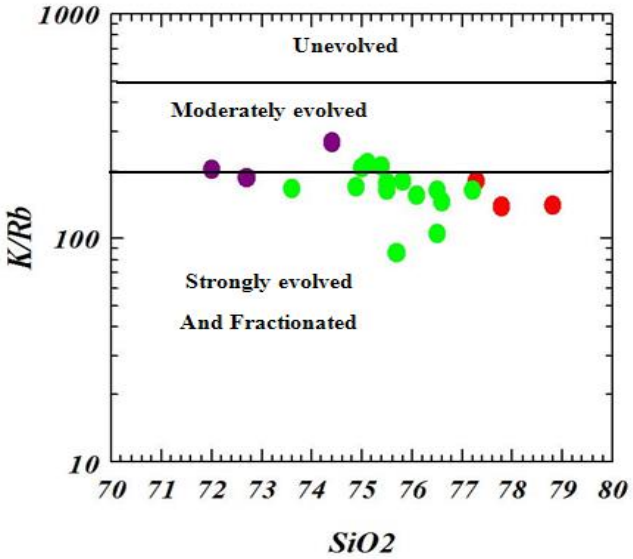

Figure 2) Location of South Mashhad granites on Blevin's K/Rb−SiO_2 diagram (Blevin, 2003). In this diagram $gr^1$and gr^2 are more differentiated and evolved than gr^3. [gr^1(●), gr^2 (●), gr^3 (●)].

These pegmatites are of the simple, homogeneous type, with an identical mineralogy and similar coarse-grained texture from the borders to the center. Their width ranges from a few centimeters to several meters and their length reaches several kilometers. The constituent minerals are:

1- Pink and white coarse-grained feldspar (up to more than 5cm long and wide) which are the dominant phases and lend their color to the entire pegmatite (Fig. 3).

2- Colorless to milky quartz with dark colored tourmaline inclusions in some areas. This assemblage is abundant at some places.

3- Silver-white to dark colored micas occurs in radial, swallow-tail and book- mica structures, (about 5cm long and wide) are present. The amount of these micas is subordinate to the feldspars; at some places quartz is the dominant mineral (Fig.4).

4- Dark to black tourmaline occurs as individual prismatic crystals or radial aggregates. The abundance of these tourmalines varies from place to place (Fig.5).

5- Red garnets can be seen as crystals ranging from a few millimeters to a few centimeters in size.

These pegmatite veins show two cross-cutting trends viz. NE-SW and NW-SE with dips ranging from N45E to N85E.

3.4–Petrography and Mineralogy of the Pegmatites

The pegmatites under study fall into the alkali feldspar granite, monzogranite to syeno-granite fields in the Streckeisen's classification (Streckeisen, 1976). Petrographic studies show that the constituent minerals of these pegmatites are: alkali feldspars, sodic plagioclase, micas (including biotite, muscovite and lepidolite) tourmaline, garnet and apatite.

Alkalifeldspars (based on petrographic studies and XRD results) are of two types: microcline and orthoclase. The microcline is mainly fresh and unaltered while the orthoclase is partly sericitized and kaolinized (Fig. 6).

Orthoclase from these pegmatites shows perthitic and micrographic textures. The plagioclases range from albite to andesine. They are unaltered to partly sericitized. The XRD results show that micas from these pegmatites are of the following types: biotite, muscovite and lepidolite. Under the microscope, the brown biotites occasionally show zircon inclusions. These biotites are in the process of alteration to tourmaline-muscovite or chlorite+iron oxide (Figs. 7a to d). The chemical formula for these biotites (based on the X-Ray results) is as follows:

$$K_2(Fe_{2.786}\,Mg_{2.321}\,Ti_{0.55})\,(Al_{2.413}\,Si_{5.587}\,O_{20})(OH)_4$$

Figure 3)Coarse grained feldspar in the pegmatites of the area which lend their colour to the entire body of the pegmatites)

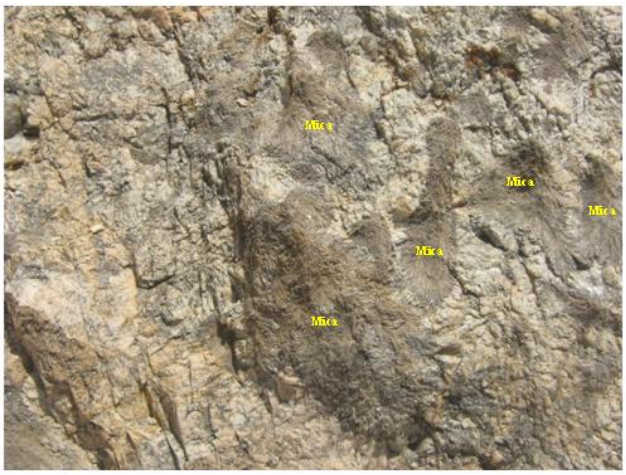

Figure 4) Coarse-grained swallow-tail shaped micas in pegmatites of the area.

Figure 5) Black tourmaline crystals pegmatites south of Mashhad (Qtz=quartz, Feld=feldspar, Mi=mica, Tour=tourmaline).

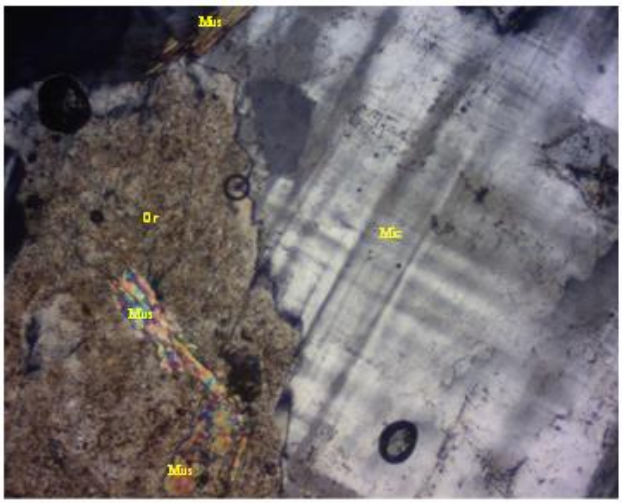

Figure 6)Tabular, unaltered microcline crystals occurring with sericitized and kaolinized orthoclase (Mus=muscovite, Or=orthoclase, Mic=microcline).

Petrographic studies show that muscovite and lepidolite are of the primary and secondary types (formed as a result of alteration of biotite and alkali feldspars). The chemical formula for these micas (based on the X-Ray results) is as follows:

-$KAl(Mn_{0.2}Al_{0.8})(Al_{0.42}Si_{3.58})O_{10}(OH)_2$- muscovite

- $KAl_2(Si_3\ Al)O_{10}(OH,\ F)_2$-muscovite

-$[K_2(Al_{2.32}Mn_{0.11}Li_{3.460})(Si_7AlO_{20})F_3(OH)]_{1.5}$- lepidolite

-$KLi(Li_{0.24}Al_{0.65})Al_{0.51}Si_{3.49}O_{10}F(OH)_{3.32}$-lepidolite

- $KLi_{1.6}Al_{2.01}Si_{3.39}O_{10}F_{1.2}(OH)_{0.8}$-lepidolite

- $KLi_{0.92}(Al_{0.55}Li_{0.35})_2Si_4O_{10}F_2$-lepidolite

-$(Al_{0.63}Li_{0.37})(Li_{0.95}Al_{0.05})(Si_{3.36}Al_{0.64})O_{10}(OH,F)_{0.5}$- lepidolite

- $KAl_2Al(Al_{0.13}Si_{3.87}O_{10})F$-lepidolite

Petrographic studies have also shown (Fig. 7) that the tourmalines from these pegmatites are of primary and secondary types (resulting from the alteration of biotite to tourmaline in the last stage of magmatic activity). XRD results on the chemical composition of these tourmalines indicate that they are of the following types: uvite (from the pneumatolytic alteration of plagioclase+biotite), elbaite, schorl and dravite.

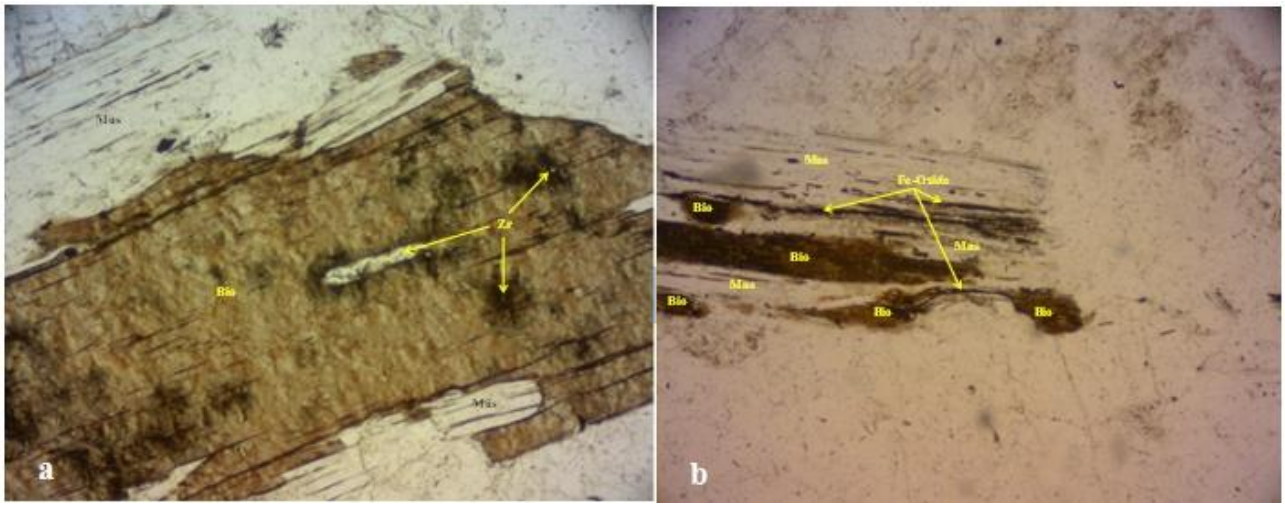

Figure 7a) Zircon inclusions surrounded by black haloes in brown biotite grains;b)Alteration of biotite tomuscovite + iron oxides(Bio=biotite, Zr=zircon, Mus=muscovite, Gar=garnet, Tur=tourmaline, Ap=apatite, Chl=chlorite).

The garnets present in thesepegmatites have been shown by SEM-EDS point analysis to be of the almandine-spessartine type (Fig. 8a). They are devoid of any zoning from the border to the center and the Fe/Mg ratio is almost constant from the border to the center (Fig. 8b).

The apatite grains are very fine grained and euhedral. SEM-EDS point analysis results indicate that they are mainly hydroxyapatite and less commonly of the fluorapatite type (Figs. 9).

4–Mineral Chemistry

4.1- Feldspars

The feldspar chemistry was investigated by ICP-OES chemical analysis which gave the following results: the Na content of these pegmatite samples ranged between 1.7% to 4.5% while the K content varied from 2.9% to 12%; the Rb content was between 351 to 967 ppm (Table 2). The average K/Rb ratio in these feldspars ranged from 126 to 152 while the Cs content was very low (<0.1 to 1.9ppm). Further, the average K/Cs ratio in these feldspars is very high (Table 2). Based on all of the presented chemical evidence we can conclude that the pegmatites under study show a low level of differentiation.

4.2- Micas

The K content of these micas varied between 3.9% to 8.5% while the Rb values lay between 361 to 1430 ppm. The Li and Cs contents ranged between 1938-6322 ppm and 2.2-6.2 ppm respectively (Table 3). The average K/Rb ratio in these micas was from 40 to 103 while the average K/Cs ratio was very high and ranged from 14810 to 16115 (Table 3).

4.3- Garnets

Point analysis data from SEM-EDS investigations and the elemental abundance data obtained for garnet grains indicate that they are

of the almandine-spessartine type with almost zero content for Mg and Ca (Fig. 10). The Fecontent of these garnets is higher than their Mn content and their composition plots near the almandine pole in the almandine-spessartine Ternary diagram (Fig. 10).

5–Geochemistry of pegmatites south of Mashhad

The pegmatites occurring south of Mashhad are peraluminous and the average A/CNK [$Al_2O_3/(CaO+K_2O+Na_2O)$] index is about 1.4and the average K_2O/Na_2O ratio is about 1.4. These pegmatites show a relatively high contents for SiO_2, K, Al, Ba, Rb, Li, Nb, and Be with lower contents for Mg, Ca, Th, U, Sm, Ti, Zr, Ta, Cs, and Fe. The Li content of these rocks varies from 202 to 1653 ppm but the average Li content is about 521 ppm (Table4).

The Mg/Li ratios for pegmatites of the Mashhad area vary from 0.2 to 12.6 (with an average value of 2.1) which indicate minimum mixing with mafic and ultramafic rocks of the area (Table 4). The average value for K/Rb ratio for these rocks is about 163 which indicate the low level of differentiation of these rocks. Similarly, the very high average Al/Ga ratio of these rocks also supports their low differentiation. The increasing trend of Li-content in these rocks is not related to the differentiation trend of the pegmatites.

Sample No.	K-Feldspars ICP-OES Analysis (ppm)											Ratio				
	Cs	Ga	Li	Al	Ca	Fe	K	Na	Sr	Ti	Rb	K/Rb	K/Cs	Rb/Sr	Rb/Cs	Al/Ga
F-1	0.90	13.3	36	105241	1121	2925	97760	18305	97.9	55.8	640	153	108622	7	711	94
F-2	0.90	14.7	44	104968	1320	1966	103889	21074	114	37.9	639	163	115432	6	710	80
F-3	0.90	20.8	135	98897	2906	4517	63873	28373	13.1	126	531	120	70970	40	590	34
F-4	0.90	14.6	68	94674	2333	2660	82112	20348	128	58.6	821	100	91235	6	912	41
F-5	0.90	16.1	76	121209	1854	2073	119761	27003	26.3	29.6	759	158	133067	29	844	65
F-6	0.90	13.1	19	111285	2159	2137	111357	21989	87.8	29.9	639	174	123730	7	709	52
F-7	0.90	11.1	61	93076	1741	2442	92945	23680	93.4	33.0	534	174	103272	6	593	53
F-8	0.90	13.4	57	95470	1004	963	103802	23486	75.2	16.9	636	163	115336	8	706	95
F-9	0.90	13.4	28	99865	3025	1037	99260	20889	53.0	16.6	749	133	110289	14	832	33
F-10	0.90	12.8	47	103007	1651	1300	94726	18292	188	33.1	522	181	105251	3	580	62
F-11	0.90	14.8	30	62059	5910	3102	46974	33653	41.9	41.1	396	119	52193	9	440	11
F-12	0.90	15.8	12	76129	1499	2414	71907	29497	12.6	18.2	681	106	79896	54	757	51
F-13	1.90	28.5	284	76801	4339	8495	29401	44756	8.61	121	484	61	15459	56	255	18
F-14	0.90	10.0	43	77799	1918	2714	72653	16602	116	174	351	207	80726	3	390	41
F-15	0.90	16.6	28	70470	3204	3683	50218	39755	39.8	111	375	134	55798	9	417	22
F-16	0.90	16.8	69	107203	699	1004	101405	23584	10.3	23.3	967	105	112672	94	1075	153
F-17	0.90	12.8	59	96352	1040	2693	89899	20918	75.6	38.2	622	145	99888	8	691	93

Table 2) Results of element analysis by ICP-OES for Potassic feldspars occurring within the pegmatites south of Mashhad.

Sample No.	Mica ICP-OES Analysis (ppm)													Ratio			
	Cs	Ga	Li	Al	Ca	Fe	K	Mg	Mn	Na	Sr	Ti	Rb	K/Rb	K/Cs	Rb/Cs	Al/Ga
M-1	4.9	103	3665	168531	721	25168	80938	5357	420	6568	9.3	2551	889	91	16641	183	1629
M-2	2.2	44.7	1938	82642	1047	12435	38675	2047	190	3111	6.0	748	361	107	17918	167	1850
M-3	6.2	116	6322	176073	630	28393	85213	3451	788	9931	1.3	634	1378	62	13785	223	1514
M-4	3.9	94.6	2144	133022	276	19915	57328	1553	345	5911	8.3	498	1430	40	14810	369	1405
M-5	5.5	98.7	5465	137254	667	26080	84233	4793	647	7295	4.6	3054	694	121	15269	126	1390
M-6	4.6	107	6030	170170	1720	18090	70956	3324	340	8689	3.4	1039	830	86	15413	180	1585

Table 3) Results of element analysis by ICP-OES for micas occurring within the pegmatites south of Mashhad.

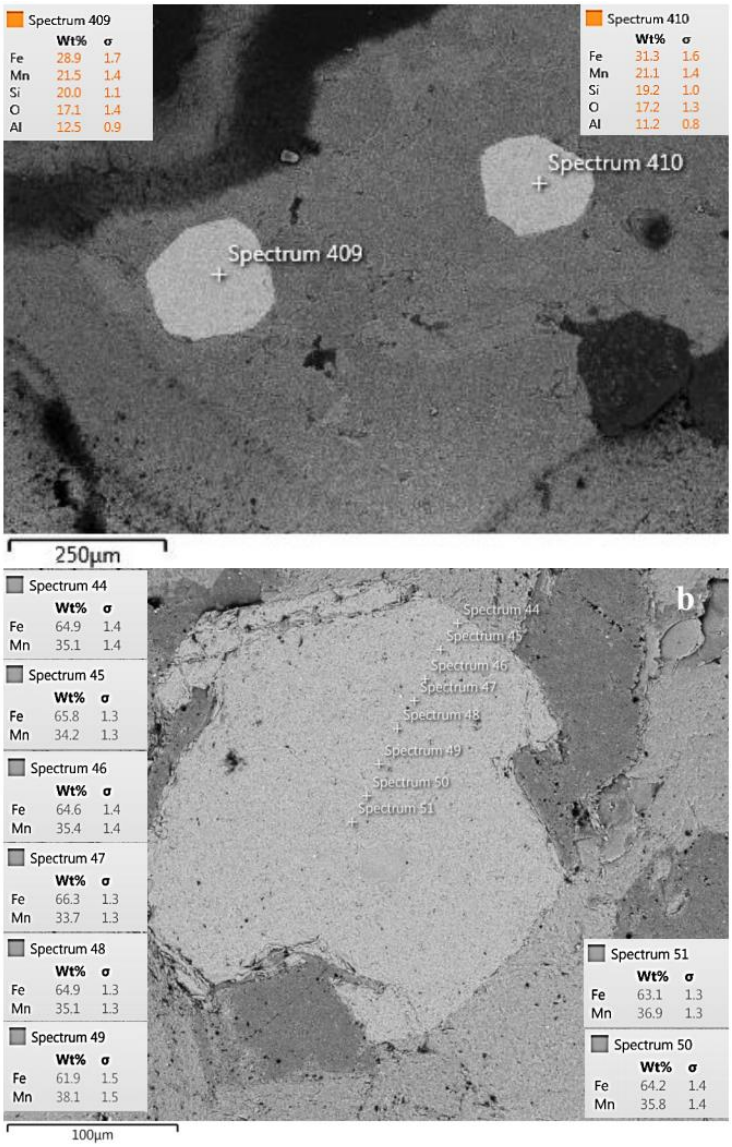

Spectrum No.	Fe (Wt%)	Mn (Wt%)	Fe/Mn
44	64.9	35.1	1.8
45	65.8	34.2	1.9
46	64.6	35.4	1.8
47	66.3	33.7	2.0
48	64.9	35.1	1.8
49	61.9	38.1	1.6
50	64.2	35.8	1.8
51	63.1	36.9	1.7

Figure 8a) Point analysis by SEM-EDS of garnets from pegmatites south of Mashhad. In these garnets their iron content is greater than their manganese content); b) Ratio of Fe/Mn in these garnets that Shown them in below table.

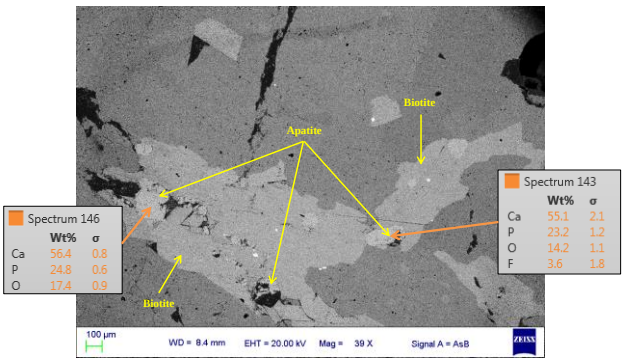

Figure 9) Point analysis by SEM-EDS of apatites in the pegmatites of the area. Mostly their composition is hydroxyl-apatite while fluor-apatite is less common.

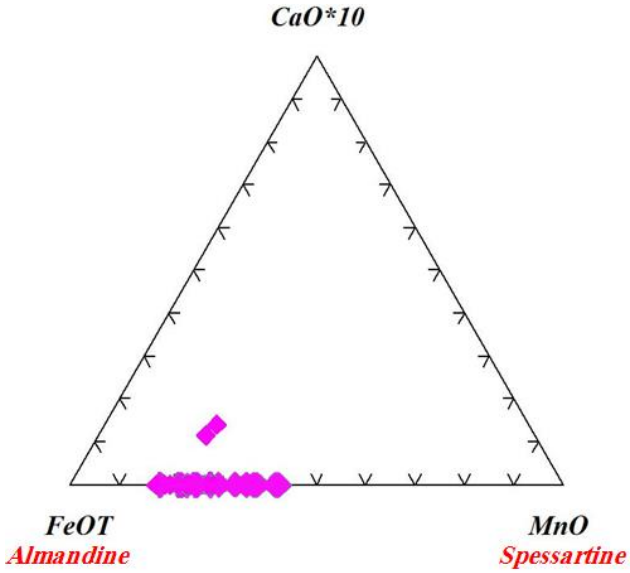

*Figure 10) Ternary diagram (Ca*10)-Mn-Fe for determination of garnet composition (after Müller et al., 2009). Garnet compositions from south of Mashhad fall on the FeO_T–MnO axis as their (Ca*10) content is very low or zero. These garnets are of the almandine-spessartine type with Fe>Mn.*

6– Fluid Inclusion Studies

Fluid inclusion studies were carried out on inclusions in quartz occurring within the pegmatites to determine the pressure and temperature conditions of their formation. Petrographic studies of the fluid inclusions from coarse grained quartz showed the distribution pattern, shape, size, number and their phase content. Most of the fluid inclusions were found as Fluid Inclusion Assemblages (FIA; Fig. 11a).

In the samples under study the fluid inclusion size varied from 8-35.5 microns showing different shapes includingrounded, angular, and irregular shapes; most commonly rounded, irregular, and occasionally elongated linear shapes were observed (Fig. 11b).

Fluid Inclusion studies carried out on these samples showed that the salinity of fluid inclusions range from 0.33 to >13 wt% NaCl with the greatest frequency of salinities occurring between 1.8 to 3.3 wt% NaCl. The salinities (wt% NaCl) and the densities were calculated using the PVTX Modeling Software for Fluid Inclusion V2.6 provided by the Linkam Company (Fig. 12a). The homogenization temperatures for the two-phase inclusions were determined by the vapor to liquid transition. The histogram of homogenization temperatures shows values ranging from 167ºC to 387ºC with the maximum frequency of homogenization temperatures occurring around 247ºC to 267ºC (Fig. 12b).

It should be noted that the heating results mentioned above have not been corrected for the effect of pressure and as such they indicate the minimum temperatures of crystallization. After the salinity and density determinations in the heating and cooling stages, the temperature of formation of the pegmatite veins was calculated by employing the Pressure-Temperature graph. The pressure of formation of these fluid inclusions was about 3000-4000 bars and their depth of formation was between 10 to 14Km below the surface level.

Sample No.	Whole Rock ICP-OES Analysis of Pegmatites (ppm)																																	Ratio								
	Al	K	Na	Ca	Fe	Mg	Mn	Ti	P	Be	Cs	Dy	Er	Eu	Ga	Gd	Li	Nb	Nd	Sm	Te	Ge	Ce	La	Rb	Sr	Pb	Zr	V	U	Th	Y	Yb	K/Rb	K/Cs	Rb/Cs	Al/Ga	Rb/Sr	Mg/Li	Th/U	A/CNK	K/Na	Fe/Mn
P-1	83654	55013	31784	5453	3967	433	102	220	245	5.6	0.9	0.2	0.1	0.2	15.9	0.2	502	10	0.8	0.2	0.2	0.2	3.0	9.0	348	74	30	14	1.0	12.6	1.4	0.8	0.1	132	64244	488	5740	10.2	0.9	0.2	1.5	1.7	39
P-2	83272	33598	34670	8323	6494	861	118	402	245	4.2	1.3	0.2	0.1	0.2	19.7	0.5	542	16	1.4	0.2	0.2	0.3	2.7	9.0	193	86	20	27	2.5	13.1	2.6	1.6	0.1	174	25738	148	4235	2.2	1.6	0.2	1.6	1.0	55
P-3	78592	31981	38282	7493	6087	361	655	71	392	9.3	1.3	0.2	0.2	0.1	13.6	0.7	252	5	2.6	0.6	0.2	0.3	7.2	9.0	165	32	33	72	1.0	15.6	3.5	10.1	1.1	194	24261	125	5792	5.2	1.4	0.2	1.5	0.8	9
P-4	100088	100108	14485	1999	1748	223	41	61	424	1.5	0.9	0.2	0.1	0.6	11.8	0.2	65	4	1.0	0.2	0.2	0.1	2.7	9.0	324	197	85	31	1.0	4.0	1.3	1.7	0.1	309	111231	360	8460	1.6	3.4	0.3	1.3	6.9	42
P-5	65555	23048	52918	9648	5053	440	111	218	211	5.3	1.2	0.2	0.1	0.1	17.9	0.6	718	12	2.2	0.6	0.2	0.1	3.7	9.0	135	62	26	9	1.0	18.4	2.9	2.3	0.1	170	18571	110	3668	2.2	0.6	0.2	1.1	0.4	46
P-6	60237	14970	39208	7049	4190	616	79	285	126	5.3	1.0	0.2	0.1	0.1	20.3	0.2	767	17	1.1	0.2	0.2	0.1	1.1	9.0	120	55	16	6	1.0	14.4	1.8	0.5	0.1	125	14956	120	2968	2.2	0.8	0.1	1.4	0.4	53
P-7	70197	43037	33996	3400	4138	282	194	79	222	10.1	1.0	0.2	0.1	0.1	18.2	0.3	398	42	0.9	0.2	0.2	0.2	1.8	9.0	391	12	29	33	1.0	12.9	1.8	3.8	0.4	134	37235	279	3853	15.8	0.7	0.2	1.2	1.3	22
P-8	57326	33511	35273	2185	3642	201	900	31	290	8.2	0.9	0.2	0.1	0.1	14.9	0.2	36	69	1.2	0.2	0.2	0.1	1.2	9.0	251	16	14	50	1.0	12.6	1.9	3.7	0.3	117	30942	265	3815	2.0	5.6	0.3	1.1	1.0	4
P-9	67216	49493	38697	5161	6969	1665	762	368	980	77.1	1.6	0.2	0.2	0.2	17.6	0.7	298	58	6.2	0.8	0.2	0.3	18.1	11.2	424	209	20	93	8.7	14.2	4.8	3.4	0.4	278	11739	42	4278	0.2	5.6	1.2	1.0	1.3	9
P-10	73429	53637	36572	19212	20904	5959	447	2214	1049	4.5	4.6	2.1	1.8	1.2	17.2	3.0	474	57	41.0	5.7	0.2	0.7	112.8	70.3	193	871	31	180	40.5	14.1	17.6	16.5	1.6	315	30495	97	4510	0.3	12.6	0.5	0.9	1.5	47
P-11	57480	42027	39085	15088	8733	1585	219	687	249	4.4	1.4	0.2	0.6	0.4	12.7	1.1	244	27	12.2	1.9	0.2	0.2	28.1	17.1	134	488	27	66	11.3	13.8	6.6	7.2	0.8	165	44554	271	5220	2.0	6.5	0.4	1.2	1.1	40
P-12	92529	73872	34400	5110	3512	292	213	120	370	9.3	0.9	0.2	0.1	0.1	13.8	0.3	832	13	1.3	0.2	0.2	0.1	2.5	9.0	458	34	34	12	1.0	13.0	1.1	2.8	0.3	157	13070	83	3580	7.4	0.4	0.4	1.0	2.1	16
P-13	68412	32223	55539	7414	10976	410	4118	160	398	9.2	2.5	0.2	0.3	0.1	19.1	1.1	610	16	2.4	0.6	0.2	0.3	6.6	9.0	205	28	21	144	1.0	19.6	7.4	17.8	2.1	62	531	9	1876	3.2	0.7	0.9	5.9	0.6	3
P-14	72687	45921	30857	8157	9009	1442	169	697	585	7.2	2.0	0.2	0.4	0.6	16.7	1.5	943	12	13.1	2.1	0.2	0.2	29.1	15.4	203	146	51	194	3.7	11.3	6.2	9.0	0.5	296	9713	33	4452	0.2	1.5	1.0	1.0	1.5	53
P-15	83247	56342	39370	25981	26142	6929	810	2616	1218	6.3	5.8	3.1	2.1	1.7	18.7	4.0	829	77	43.9	7.6	0.2	1.0	135.5	73.4	190	997	23	140	51.8	16.2	15.5	21.9	2.1	169	35164	208	4570	6.6	8.4	0.2	1.5	1.4	32
P-16	77937	41080	30384	2569	3935	235	190	90	409	76.3	1.0	0.2	0.1	0.1	17.4	0.2	359	120	0.2	0.2	0.2	0.3	1.1	9.0	427	83	22	36	1.0	11.9	2.7	0.7	0.1	96	39340	408	4480	5.2	0.7	0.2	1.6	1.4	21
P-17	82573	37169	33548	3453	4383	327	106	86	296	11.7	0.9	0.2	0.1	0.1	16.8	0.2	368	27	0.2	0.2	0.2	0.3	1.3	9.0	256	19	35	22	1.0	12.6	2.2	0.6	0.1	145	41299	284	4908	13.3	0.9	0.2	1.6	1.1	41
P-18	81158	41722	32378	1789	7345	441	1303	91	304	18.4	1.3	0.2	0.1	0.1	13.4	0.6	272	26	0.2	0.2	0.2	0.4	1.3	9.0	271	24	41	37	1.0	11.2	3.4	5.7	0.5	154	32203	209	6056	11.2	1.6	0.3	1.6	1.3	6
P-19	64014	19872	37296	4834	5502	402	300	96	250	23.1	1.2	0.2	0.1	0.1	11.1	0.4	202	5	0.9	0.2	0.2	0.2	1.5	9.0	104	31	23	21	1.0	13.0	2.6	2.3	0.3	191	16782	88	5761	3.4	2.0	0.2	1.5	0.5	18
P-20	72503	34251	37171	7064	11923	550	2784	177	232	141.7	2.5	0.2	0.2	0.1	21.8	1.0	505	28	1.0	0.2	0.2	0.4	2.3	9.0	138	23	16	56	1.0	13.5	4.2	8.5	0.8	182	13701	75	3319	8.3	1.1	0.3	1.4	0.9	4
P-21	73442	42077	39415	3920	3653	380	221	129	301	21.8	0.9	0.2	0.1	0.1	15.4	0.2	479	21	0.8	0.2	0.2	0.3	1.6	9.0	312	32	28	30	1.0	13.8	1.6	2.4	0.1	171	65069	380	5602	3.1	0.8	0.3	1.5	1.1	17
P-22	60292	31647	23678	3177	5555	673	149	187	316	5.7	0.9	0.2	0.2	0.1	13.2	0.5	525	16	1.9	0.4	0.2	0.1	2.2	9.0	137	28	22	15	1.0	8.0	2.0	3.1	0.1	162	107549	663	7734	16.6	1.3	0.1	1.1	1.3	37
P-23	91166	96794	22848	1751	2916	150	98	27	992	4.1	0.9	0.2	0.1	0.1	11.8	0.2	220	3	0.6	0.2	0.2	0.2	1.8	9.0	597	36	62	11	1.0	8.5	0.9	1.3	0.1	161	82080	509	6702	13.6	0.7	0.1	1.2	4.2	30
P-24	74041	22690	36052	7388	6116	675	276	340	198	12.1	1.1	0.2	0.1	0.1	18.4	0.6	669	26	1.9	0.2	0.2	0.2	6.8	9.0	154	54	18	23	1.0	13.5	3.1	4.5	0.5	147	20877	141	4014	2.8	1.0	0.2	1.6	0.6	22
P-25	81465	58562	21575	3695	4230	580	166	186	273	6.0	0.9	0.2	0.1	0.3	14.5	0.3	414	11	1.2	0.2	0.2	0.3	3.4	9.0	342	112	42	39	1.0	7.8	2.5	3.8	0.3	115	67244	584	3990	60.0	1.4	0.1	1.3	2.7	25
P-26	91929	64560	24760	4339	3436	586	77	359	382	6.5	0.9	0.2	0.2	0.4	14.7	0.3	400	13	1.1	0.4	0.2	0.1	4.9	9.0	324	115	50	25	1.0	9.0	1.4	3.9	0.3	226	23029	102	4360	1.4	1.5	0.6	1.3	2.6	44
P-27	89382	57820	27741	3542	4504	300	436	112	278	6.1	0.9	0.2	0.1	0.1	15.6	0.2	493	9	0.3	0.2	0.2	0.2	1.7	9.0	439	43	35	32	1.0	9.4	1.7	4.6	0.5	132	64244	488	5740	10.2	0.6	0.2	1.5	2.1	9
P-28	91534	53030	28551	4791	4720	635	90	232	222	3.6	0.9	0.2	0.1	0.1	22.5	0.4	718	19	0.2	0.2	0.2	0.4	2.3	9.0	374	48	25	30	1.0	11.7	2.4	2.8	0.1	142	58922	415	4067	7.8	0.9	0.2	1.6	1.9	53
P-29	73085	40039	42357	5568	3773	249	259	68	338	4.4	0.9	0.2	0.1	0.1	13.8	0.5	575	7	1.9	0.8	0.2	0.1	4.9	9.0	230	18	18	19	1.0	14.9	2.0	5.0	0.5	174	44488	255	5297	12.4	0.4	0.1	1.2	0.9	15
P-30	80109	39811	32495	4210	9937	750	620	180	186	6.5	2.0	0.2	0.1	0.1	29.0	0.7	1080	85	1.0	0.3	0.2	0.4	1.9	9.0	470	11	11	31	4.1	12.5	3.9	2.7	0.3	85	20071	237	2762	43.8	0.7	0.3	1.6	1.2	16
P-31	70058	37181	37415	3846	5466	1154	848	121	254	7.0	1.1	0.2	0.1	0.1	19.4	0.4	523	27	1.0	0.2	0.2	0.1	2.1	9.0	244	6	10	73	1.0	13.1	2.5	5.1	0.6	152	35338	232	3620	41.5	2.2	0.2	1.3	1.0	6
P-32	81642	48554	28410	4754	4607	401	126	92	244	7.1	0.9	0.2	0.1	0.1	16.1	0.4	374	13	1.9	0.4	0.2	0.3	4.4	9.0	329	31	28	48	1.0	10.5	2.7	3.2	0.3	148	53948	365	5072	10.5	1.1	0.3	1.5	1.7	36
P-33	59415	40448	38533	3688	5748	251	1178	80	286	24.8	1.2	0.2	0.1	0.1	18.0	0.5	445	33	1.3	0.6	0.2	0.2	2.7	9.0	335	9	23	59	1.0	13.3	3.2	11.3	1.3	121	33934	281	3305	36.9	0.6	0.2	1.1	1.0	5
P-34	60171	27242	38617	6331	8808	350	2437	89	286	10.6	1.7	0.2	0.4	0.1	17.3	0.9	372	12	1.4	0.3	0.2	0.2	4.6	9.0	228	16	19	90	1.0	13.6	4.2	23.6	2.8	120	15928	133	3473	14.2	0.9	0.3	1.2	0.7	4
P-35	63921	43595	35685	5485	5805	271	1052	165	237	179.0	1.0	0.2	0.1	0.1	19.3	0.5	386	111	3.3	0.6	0.2	0.2	6.2	9.0	355	28	16	51	1.0	12.4	3.8	5.3	0.3	123	43160	351	3308	12.6	0.7	0.3	1.1	1.2	6
P-36	80947	46804	34401	18158	22862	5721	557	2123	2172	4.4	4.5	5.1	1.7	1.1	17.7	3.5	523	39	25.1	4.2	0.2	0.7	76.5	45.2	139	595	44	197	36.4	14.0	14.7	25.1	2.0	247	10308	42	4561	0.3	10.9	1.1	1.2	1.4	41
P-37	54597	28530	39435	5697	7091	129	2407	62	208	7.4	1.6	0.5	0.4	0.1	15.4	0.7	262	9	1.3	0.2	0.2	0.3	2.2	9.0	186	16	17	58	1.0	13.6	3.1	22.7	2.5	154	17939	117	3552	11.9	0.5	0.2	1.1	0.7	3
P-38	37794	22541	49842	3810	4653	132	758	77	265	6.3	0.9	0.2	0.1	0.1	18.3	0.3	509	37	2.6	0.2	0.2	0.1	0.4	9.0	186	2	9	47	1.0	17.8	2.4	4.1	0.5	121	25045	207	2063	86.9	0.3	0.1	0.7	0.5	6
P-39	53094	23945	45869	2858	4236	280	152	94	487	9.2	0.9	0.2	0.1	0.1	20.5	0.2	1653	39	0.5	0.2	0.2	0.1	0.4	9.0	260	2	6	14	1.0	16.0	1.6	1.2	0.1	92	26806	289	2585	117.5	0.2	0.1	1.1	0.5	28
P-40	45667	35673	42306	2610	4671	165	1055	41	396	5.9	1.0	0.2	0.1	0.1	17.8	0.3	965	22	0.4	0.2	0.2	0.1	1.1	9.0	351	2	6	36	1.0	14.8	1.9	5.1	0.6	135	46753	347	4782	9.9	0.2	0.1	1.3	0.8	4
P-41	73258	60520	23808	1288	3941	481	330	147	384	7.2	0.9	0.2	0.1	0.1	18.4	0.2	322	31	1.1	0.2	0.2	0.2	1.9	9.0	525	9	31	32	1.0	7.8	0.9	2.4	0.2	110	42246	384	3852	32.4	1.5	0.1	1.3	2.5	12
P-42	85062	54115	40741	7602	4826	800	164	315	585	13.4	1.2	0.2	0.2	0.4	16.3	0.8	460	28	8.5	1.0	0.2	0.2	22.1	12.2	329	161	38	82	3.9	13.9	5.2	6.2	0.5	199	71733	360	6261	2.8	1.7	0.2	1.5	1.3	29
Average	72957	43787	35249	6188	6817	923	646	333	423	19.1	1.5	0.4	0.3	0.2	17.0	0.7	514	30	4.6	0.8	0.2	0.3	12.4	13.3	284	116	27	52	4.7	12.8	3.8	6.4	0.6	162	37909	252	4482	15.5	2.1	0.3	1.4	1.4	24

Table 4)Results of element analysis by ICP-OES (including elemental ratios) for whole rock pegmatite samples from the pegmatites south of Mashhad.

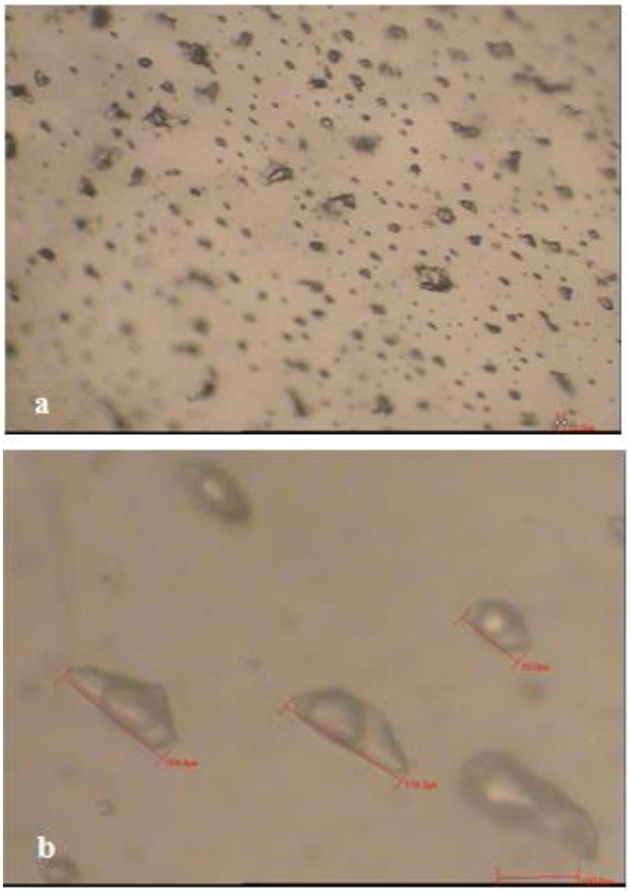

Figure 11a) Photomicrograph of Fluid inclusions in quartz from the pegmatites of the area seen as Fluid Inclusion Assemblage (FIA); b) Photo micrograph showing the size and shape of fluid inclusions (usually irregular or elongated) in quartz from the pegmatites of the area.

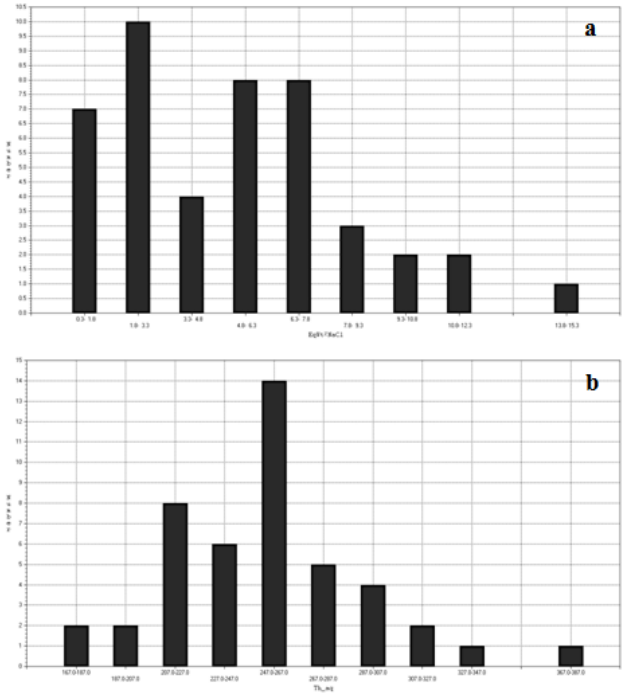

Figure 12a)Histogram of the salinity of the fluid inclusions ranging from 0.33 to more than 13wt% NaCl. The maximum vales are between 1.8–3.3 wt% NaCl; b) Histogram of homogenization temperatures ranging from 167 to 387°C showing the maximum for homogenization temperatures occurring between 247–267°C.

7–Conclusions

The pegmatites of south of Mashhad are homogeneous with a simple mineralogical composition containing alkali feldspars (microcline and orthoclase), quartz and micas (muscovite and lepidolite). Other constituent minerals in these pegmatites include plagioclase (albite to andesine), biotite, tourmaline (elbaite, dravite and schorl) and garnets (almandine-spessartine). As shown by the mineralogical composition and the high Li-content of these pegmatites they belong to the MSREL-Li type (Muscovite-Rare Element-Lithium). The K/Rb and K/Cs ratios for these pegmatites are high which indicates their low level of differentiation. The Cs-content in the alkali feldspars from these pegmatites is very low (1 to1.9 ppm) and the Li content in the white micas is rather high. Garnets from these pegmatites have iron content higher than the manganese content and they tend towards the almandine pole in the Fe-Mngarnet diagram.The pegmatites south of Mashhad are peraluminous and the average A/CNK ratio in theses rocks is about 1.4. These pegmatites show a low level of differentiationas the average K/Rb ratio is very high (~ 163). Similarly, the Al/Ga ratio in these rocks is very high.Finally, the pegmatites are lepidolite-bearing. The Li-content of these pegmatites varies from 202-1653 ppm and they have been reported for the first time from Iran in this paper. In view of the ever-increasing demand for lithium by the industry, the pegmatite field deserves further study in the future.

Acknowledgments:

Hereby we thank Dr. A. Lima and Dr. D. Stijn for their valuable comments which help us to improve the manuscript.

References:

Alavi, M. 1991. Tectonic map of the Middle East, Geological Survey of Iran.

Blevin, P.L. 2003. Metallogeny of granitic rocks. pp. 1–4 In: Blevin P., Jones M. and Chappell B. eds. Magmas to mineralisation: the Ishihara symposium. Geoscience Australia Record 2003/14.

Černý, P. 1989. Mineralogy of rubidium and cesium. In: Černý P (ed) Anatomy and classification of granitic pegmatite in science and industry. Mineralogical Association of Canada. Short Course Handbook: 8, 1–39.

Černý, P., Ercit, T. 2005. The classification of granitic pegmatite revisited, The Canadian Mineralogist: 43, 2005–2026.

Didar, P. 2003. Petrology of the granitoids of south Mashhad, with special focus on the geochemistry of their REE, unpublished M.Sc. thesis, Research Institute for Earth Sciences, Geological Survey and Mineral Exploration of Iran (in Persian).

Emami, M. H. 2000. Magmatism in Iran, Geological Survey and Mineral Exploration of Iran, 405-429, 608 pages (in Persian).

Guilbert, J. M., Park, C. F. 1997. The Geology of Ore Deposits. New York, Freeman.

Karimpour, M. H., Farmer, G. L., Stern, C. R. 2009. Geochronology, radiogenic isotope geochemistry, and petrogenesis of Sangbast Paleo-Tethys monzogranite, Mashhad, Iran, Journal of Iranian Society of Crystallography and Mineralogy: 14, 706–719.

Karimpour, M. H., Farmer, G. L., Stern, C. R. 2011. Geochemistry of Rb-Sr and Sm-Nd, radiometry of U-Pb zircon, and provenance of leucogranites of KhajehMorad, Mashhad, Iran. Quarterly Journal of Earth Sciences: 80, 171–182 (in Persian).

Muller, A., Ihlen, P.M, R. B. Larsen, Spratt, J., Seltmann, R. 2009. Quartz and Garnet Chemistry of South Norwegian Pegmatite and its implications for Pegmatite Genesis. Estudos Geologicos: 19, 20–24.

Streckeisien, A. T. 1976. To each plotonic rock its proper name. Earth Sciences Reviews: 12, 1–33.

Taheri, J., Ghaemi, F. 1994. 1:100,000 geological map of Mashhad, Geological Survey of Iran.

Valizadeh, M., Karimpour, M. H. 1995. Provenance and tectonic setting of the south Mashhad granites. Journal of Science, University of Tehran: 21, 71–82 (in Persian).